Research Article | Vol. 28, No. 6 / 16 March 2020 / Optics Express 8475
Optics EXPRESS

Vortex preserving statistical optical beams

ZHIHENG XU,[1,2] XIAOFEI LI,[1,2] XIN LIU,[1,2] SERGEY A. PONOMARENKO,[3,4] YANGJIAN CAI,[1,2,5,6] AND CHUNHAO LIANG[1,2,3,7]

[1]*Shandong Provincial Engineering and Technical Center of Light Manipulation & Shandong Provincial Key Laboratory of Optics and Photonic Devices, School of Physics and Electronics, Shandong Normal University, Jinan 250014, China*
[2]*Collaborative Innovation Center of Light Manipulations and Applications, Shandong Normal University, Jinan 250358, China*
[3]*Department of Electrical and Computer Engineering, Dalhousie University, Halifax, Nova Scotia B3J 2X4, Canada*
[4]*Department of Physics and Atmospheric Science, Dalhousie University, Halifax, Nova Scotia B3H 4R2, Canada*
[5]*School of Physical Science and Technology, Soochow University, Suzhou 215006, China*
[6]*yangjiancai@suda.edu.cn*
[7]*cliang@dal.ca*

Abstract: We establish a general form of the cross-spectral density of statistical sources that generate vortex preserving partially coherent beams on propagation through any linear ABCD optical system. We illustrate our results by introducing a class of partially coherent vortex beams with a closed form cross-spectral density at the source and demonstrating the beam vortex structure preservation on free space propagation and imaging by a thin lens. We also show the capacity of such vortex preserving beams of any state of spatial coherence to trap nanoparticles with the refractive index smaller than that of a surrounding medium.

1. Introduction

The concept of vortices was first introduced into optics by Coullet in 1989 [1] by analogy with the naturally encountered vortices, such as tornados and ocean whirlpools. This work was followed by a rigorous introduction of vortex-carrying optical beams with helicoidal wavefronts by Allen and co-workers [2]. The introduced vortex beams were shown in [2] to carry orbital angular momenta of $m\hbar$ per photon where m is an integer known as a topological charge of the vortex. This pioneering work has established a link between an optical vortex on the one hand and the beam orbital angular momentum on the other, thereby having triggered a flurry of research on vortex beams [3,4]. A multitude of noteworthy features of optical vortex beams have been discovered to date. The latter include the phase singularity behavior of vortex beams; their ability to transfer the orbital angular momentum to neutral particles, thereby enabling trapping and tweezing the said particles, as well as an angular Doppler effect manifestation with vortex endowed beams [5,6]. These remarkable characteristics of optical vortex beams serve as a basis for their widespread applications to high-security and high-capacity quantum and classical optical communications, quantum storage, nanostructure processing, and superresolution imaging [7–9], to mention but a few relevant examples.

On the other hand, as the source coherence is reduced, fully spatially coherent vortex beams can be converted into partially coherent vortex beams (PCVBs) [10,11]. In general, partially coherent beams have been demonstrated to better resist ambient turbulence fluctuations than do their fully coherent counterparts [12], and are useful for diffractive imaging [13]. In this connection, PCVBs have received much attention, in part due to their interesting propagation properties such as self-shaping, self-reconstruction, and reduced turbulence-induced degradation

#387181 https://doi.org/10.1364/OE.387181
Journal © 2020 Received 2 Jan 2020; revised 28 Feb 2020; accepted 28 Feb 2020; published 9 Mar 2020

Optics EXPRESS

and scintillations [10,11]. However, traditional partially coherent vortices, embedded within Schell-model beams [14–16], lose their vortex structure on free space propagation, especially in the low-coherence limit where their structural stability to random environment fluctuations is the greatest. Hence a natural question arises: Is it possible to combine the advantages of low spatial coherence, and hence the structural stability to ambient turbulence, and optical vortex structure by generating PCVBs whose vortex structure is immune to beam evolution through a linear ABCD system, including free space, at any spatial coherence level? Several groups have proposed particular classes of PCVBs satisfying this requirement [17–19]. To the best of our knowledge, however, no general approach to designing vortex preserving partially coherent beams (PCBs) has been put forward to date. Nor have any applications of such beams been explicitly discussed.

In this work, we establish, for the first time to our knowledge, a general form of the cross-spectral density of PCVBs that maintain their vortex structure on propagation though any linear ABCD optical system. In particular, we demonstrate how any such beam can be constructed using coherent pseudo-modes. This, in general pseudo-mode, decomposition offers a direct path to the laboratory realization of such beams [18]. We also introduce a class of vortex preserving partially coherent beams described by the cross-spectral density in a closed form. We then calculate the radiation forces due to the optical fields of such beams that enable nanoparticle trapping in the beam cores.

2. General form of vortex preserving partially coherent beams

In the space-frequency domain, the cross-spectral density (CSD) is used to characterize the second-order statistical properties of a PCB. To establish a generic form of vortex preserving PCBs, we introduce the CSD of a random ensemble $\{U(\boldsymbol{\rho}, \omega)\}$ at the source as

$$W^{(0)}(\boldsymbol{\rho}_1, \boldsymbol{\rho}_2, \omega) = \langle U^*(\boldsymbol{\rho}_1, \omega)\, U(\boldsymbol{\rho}_2, \omega)\rangle, \tag{1}$$

where $\boldsymbol{\rho} = (\rho, \varphi)$ is a radius vector in the transverse plane and the angle brackets denote ensemble averaging. We construct the ensemble as follows

$$U(\rho, \varphi) = e^{im\varphi} \sum_n c_n \psi_{mn}(\rho), \tag{2}$$

where m is an integer and we drop the frequency dependence for brevity hereafter. Further, $\{\psi_{mn}(\rho)\}$ are, in general, pseudo-modes in the spirit of [20–25] as they can fail to form an orthogonal set. Such pseudo-modes were shown to be instrumental for design and experimental realization of novel classes of partially coherent beams [21–24,26–29] and for theoretical explorations into statistical surface plasmon polaritons [30,31] as well as they were demonstrated to provide insight into partially coherent beam propagation in linear graded-index media [32], turbulent atmosphere [33], and uniaxial crystals [34]. Next, $\{c_n\}$ are random coefficients with the second-order statistical properties encapsulated by

$$\langle c_n^* c_l \rangle = \lambda_n \delta_{nl}. \tag{3}$$

Here $\{\lambda_n \geq 0\}$ are essentially non-negative modal weights of the Karhunen-Loève expansion of the random field in terms of the pseudo-modes $\{\psi_{mn}\}$. The corresponding coherent-mode decomposition follows at once from Eqs. (1) through (3) as

$$W^{(0)}(\boldsymbol{\rho}_1, \boldsymbol{\rho}_2) = e^{im(\varphi_2 - \varphi_1)} \sum_n \lambda_n \psi_{mn}^*(\rho_1)\, \psi_{mn}(\rho_2). \tag{4}$$

Optics EXPRESS

The propagation properties of such beams through an ABCD optical system can be studied with the help of the following extended Huygens-Fresnel diffraction integral formula

$$W(\mathbf{r}_1,\mathbf{r}_2,z) = \frac{k^2}{4\pi^2B^2}\int d^2\boldsymbol{\rho}_1\int d^2\boldsymbol{\rho}_2 W^{(0)}(\boldsymbol{\rho}_1,\boldsymbol{\rho}_2)\exp\left[-\frac{ik}{2B}\left(A\boldsymbol{\rho}_1^2-2\mathbf{r}_1\cdot\boldsymbol{\rho}_1+D\mathbf{r}_1^2\right)\right] \times\exp\left[\frac{ik}{2B}\left(A\boldsymbol{\rho}_2^2-2\mathbf{r}_2\cdot\boldsymbol{\rho}_2+D\mathbf{r}_2^2\right)\right]. \tag{5}$$

Here $\mathbf{r}=(r,\phi)=(x,y)$ is the transverse vector in any plane $z\geq 0$; $k=2\pi/\lambda$ stands for the wave number, with λ denoting the carrier wavelength of light. It follows from Eqs. (4) and (5) that

$$W(\mathbf{r}_1,\mathbf{r}_2,z)=\sum_n \lambda_n\psi_{mn}^*(\mathbf{r}_1,z)\psi_{mn}(\mathbf{r}_2,z), \tag{6}$$

where

$$\psi_{mn}(\mathbf{r},z)=\frac{k}{2\pi B}\int d^2\boldsymbol{\rho}\, e^{im\varphi}\psi_{mn}(\rho)\exp\left[\frac{ik}{2B}\left(A\boldsymbol{\rho}^2-2\mathbf{r}\cdot\boldsymbol{\rho}+D\mathbf{r}^2\right)\right]. \tag{7}$$

On performing the angular integration in the polar coordinates in Eq. (7) using the integral representation of the Bessel function of the first kind and order m as

$$J_m(x)=\int_0^{2\pi}\frac{d\varphi}{2\pi}\exp(im\varphi-ix\cos\varphi), \tag{8}$$

we obtain, upon elementary algebra, the expression for a coherent mode field in any transverse plane $z\geq 0$ in the form

$$\psi_{mn}(r,\phi,z)=\left(\frac{k}{B}\right)\exp\left(\frac{ikDr^2}{2B}\right)e^{im\phi}R_{mn}(r), \tag{9}$$

where

$$R_{mn}(r)=\int_0^\infty d\rho\,\rho\,\psi_{mn}(\rho)\,J_m\left(\frac{kr\rho}{B}\right)\exp\left(\frac{ikA\rho^2}{2B}\right). \tag{10}$$

It follows at once from Eq. (9) that each coherent mode has a vortex phase in any $z\geq 0$ with the **same topological charge** m and its radial profile $R_{mn}(r)$ vanishes on the axis $r=0$ for any nonzero topological charge $m>0$ because of the factor $J_m(kr\rho/z)$ in the integrand on the right-hand side of Eq. (10). Hence, each mode carries a vortex with the same topological charge, implying the overall beam is endowed with the optical vortex in any transverse plane. As a consequence, each (pseudo-)mode maintains a dark notch in its intensity profile on propagation through any linear ABCD system, thereby ensuring that the overall beam intensity possesses the notch as well, which makes it a signature of any vortex-preserving PCVB.

We have now established the general form of the CSD, given by Eqs. (6), (9) and (10), of a statistical source generating vortex endowed PCBs that maintain their vortex structure on propagation through a generic ABCD optical system. Next, we proceed to introduce a class of such beams with a closed form CSD at the source to illustrate our general results.

3. New class of vortex preserving statistical beams

Consider a class of radially sinc-correlated vortex (RSCV) beams with the cross-spectral density in a closed form as

$$W_{\text{sinc}}^{(0)}(\boldsymbol{\rho}_1,\boldsymbol{\rho}_2)=I_0(\rho_1\rho_2)^{|m|}e^{im(\varphi_2-\varphi_1)}\exp\left[-\frac{(\rho_1^2+\rho_2^2)}{2\sigma_1^2}\right]\text{sinc}\left(\frac{\rho_1-\rho_2}{\sigma_c}\right), \tag{11}$$

Optics EXPRESS

where I_0 is a positive normalization constant; σ_I and σ_c denote the beam width and coherence width of any RSCV beam, respectively. Using the following sinc-function representation [35]

$$\operatorname{sinc}(x-y)=\frac{\pi}{\sqrt{xy}}\sum_{n=0}^{\infty}(n+1/2)\,J_{n+1/2}(x)\,J_{n+1/2}(y), \tag{12}$$

we can easily read off the pseudo-modes to be

$$\psi_{mn}(\rho,\varphi)=\rho^{|m|-1/2}e^{im\varphi}e^{-\rho^2/2\sigma_I^2}J_{n+1/2}(\rho/\sigma_c), \tag{13}$$

and the set of eigenvalues $\{\lambda_n\}$ reads as

$$\lambda_n=\pi\sigma_c I_0(n+1/2). \tag{14}$$

On substituting from Eqs. (13) and (14) into Eq. (7), we obtain after somewhat tedious algebra, the pseudo-modes of an RSCV beam at the propagation distance z within a linear ABCD optical system, with the following analytical expression for $R_{mn}(r)$

$$\begin{aligned}R_{mn}(r)=&\frac{(kr/B)^m h^{-(m+|m|+n+2)/2}}{\sigma_c^{n+1/2}2^{m+n+3/2}\Gamma(n+3/2)}\sum_{s=0}^{\infty}\frac{\Gamma[s+(m+|m|+n+2)/2]}{s!\Gamma(s+n+1)}\left(-\frac{k^2r^2}{4B^2h}\right)^s\\&\times F\left(-s,-n-s;n+3/2;B^2/k^2r^2\sigma_c^2\right).\end{aligned} \tag{15}$$

Here $h=1/2\sigma_I^2-ikA/2B$, Γ stands for a Gamma function; $F(\alpha,\beta;\gamma;z)={}_2F_1(\alpha,\beta;\gamma;z)$ denotes a Gauss hypergeometric function, ${}_pF_q\left(\alpha_1,\alpha_2,\ldots,\alpha_p;\gamma_1,\gamma_2,\ldots,\gamma_q,;z\right)$ being a generalized hypergeometric series [35]. We take 30 modes in the following numerical simulations. We checked that the increase in the mode number beyond 30 does not alter our results.

In the remainder of the paper, we adopt the modified free-space geometry whereby the beam, focused by a thin lens with focal length f=600mm, propagates toward a receiver plane. The distances from the lens to the source and receiver planes are f and z, respectively. For this optical system, the corresponding elements of the transfer *ABCD* matrix can be expressed as

$$A=1-z/f,\quad B=f,\quad C=-1/f,\quad D=0. \tag{16}$$

Applying Eqs. (6), (9), (14) and (15), we can obtain the intensity distributions $I(\mathbf{r},z)=W(\mathbf{r},\mathbf{r},z)$ of RSCV beams at the different propagation distances from the source plane. In Fig. 1, we exhibit intensity evolution of RSCV beams with the carrier wavelength of 632.8 nm and different topological charges m at several propagation distances from the source, $z=0.6f$, $z=0.8f$ and $z=f$. We infer from the figure that the hollow dark cores of RSCV beams are maintained on the beam propagation all the way to the focal plane of the lens located in the far-zone of the source. It follows that the RSCV beam vortex structure remains intact as predicted by Eqs. (6), (9), and (10). Importantly, our conclusions can be extended to RSCV beams with any topological charge m as is illustrated by different l rows of Fig. 1.

To further illustrate the vortex structure preservation of RSCV beams, we study the focal plane ($z=f$) intensity distributions of such beams with different topological charges m generated by sources of different states of coherence that are characterized by the source coherence width σ_c. We display the relevant numerical results in Fig. 2. To show the effect of the source coherence width σ_c on the vortex structure, we plot the corresponding cross lines $I(x,y=0)/I_{\max}(x,y=0)$ of normalized RSCV beam intensity distributions in three cases: $\sigma_c=1$mm (black), $\sigma_c=0.5$mm (red), and $\sigma_c=0.1$mm (green) as well. We stress that our results indicate the vortex structure preservation in the focal plane for the RSCV beams with any topological charges m even in the low coherence limit, $\sigma_c\ll\sigma_I$. We can see from the right l column in the figure that the source coherence has little effect on the central portion of the beams for all topological charges m, even

Optics EXPRESS

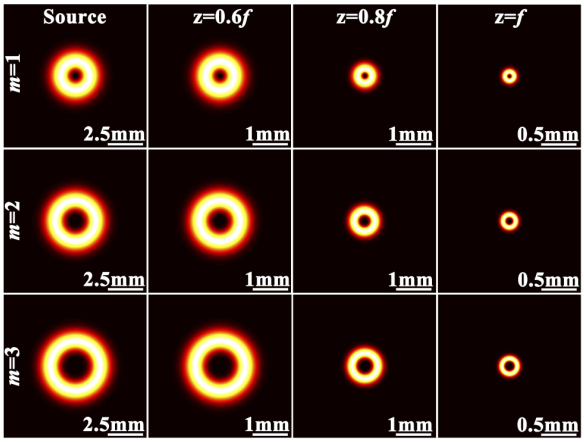

Fig. 1. Evolution of the RSCV beam intensity distributions focused by a thin lens at several propagation distances. The beam intensity is normalized by its peak intensity. The numerical parameters are as follows: $\sigma_I = 1$mm and $\sigma_c = 1$mm. White horizontal lines in each graphic array l indicate a spatial scale within the l.

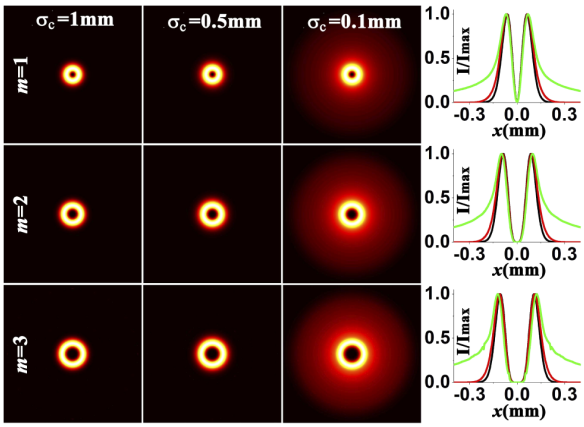

Fig. 2. Intensity distributions of radially sinc-correlated vortex beams in the focal plane (i.e., $z = f$) with different topological charges m and the source coherence width σ_c. In the right l column, the corresponding cross lines $I(x, y = 0)/I_{\max}(x, y = 0)$ of such beams with $\sigma_c = 1$mm (black), $\sigma_c = 0.5$mm (red), and $\sigma_c = 0.1$mm (green) are exhibited. The root mean square source width is taken to be $\sigma_I = 1$mm.

though it strongly influences the power distribution in the beam tails. Thus, the vortex structure resilience on propagation of nearly incoherent RSCV beams through any linear ABCD system makes such beams quite different from typical PCVBs [10].

As is well known, whenever vortex beams are scattered by a small obstacle, a neutral dielectric sphere, for example, the momentum of the beam and the sphere are exchanged, giving rise to radiation and scattering forces pushing the sphere to a stable equilibrium position within the beam field. This phenomenon lies at the heart of optical trapping of small particles [3]. In the following section, we discuss the trapping forces exerted by sinc-correlated vortex beams onto a small spherical particle.

Optics EXPRESS

4. Trapping dielectric nanoparticles with radially sinc-correlated vortex beams

We now consider a spherical dielectric nanoparticle of radius a that we assume to be much smaller than the carrier wavelength of the beam, $a \ll \lambda$. In this approximation, we can adopt the Rayleigh scattering theory [36] to analyze the radiation forces experienced by the nanoparticle in the field of an RSCV beam. A detailed analysis [25,37] shows that the scattering and gradient forces are the leading forces experienced by the particle in the radiation filed, whereas the gravitational, buoyancy, drag, and Brownian forces are negligible in comparison. Hence, we only take the scattering and radiation forces into consideration in this work.

We assume the RSCV beam, focused by a thin lens with the focal length f, to propagate toward a receiver plane. Further, the distances from the lens to the source plane and to the receiver plane are assumed to be l and z, respectively. The corresponding ABCD transfer matrix can then be expressed as

$$\begin{pmatrix} A & B \\ C & D \end{pmatrix} = \begin{pmatrix} 1 - z/f & l + z - lz/f \\ -1/f & 1 - l/f \end{pmatrix}. \tag{17}$$

It follows from the Rayleigh scattering theory that the scattering force is given by the expression [25,36,37]

$$\mathbf{F}_{scat}(r, \phi, z) = \frac{8\pi}{3c} n_2 (ka)^4 a^2 \left(\frac{n_r^2 - 1}{n_r^2 + 2} \right)^2 I(r, \phi, z)\, \mathbf{e}_z. \tag{18}$$

Here c is the speed of light in vacuum; $n_r = n_1/n_2$ is a relative refractive index, with n_1 and n_2 being the refractive indices of the nanoparticle and surrounding medium, respectively, and $\mathbf{e}_z$ is a unit vector along the beam propagation axis. Next, the gradient force can be shown to read [25,36,37]

$$\mathbf{F}_{grad}(r, \phi, z) = \frac{2\pi}{c} n_2 a^3 \frac{n_r^2 - 1}{n_r^2 + 2} \nabla I(r, \phi, z). \tag{19}$$

The gradient force pushes the nanoparticle to the maximum or minimum intensity area, depending on whether the relative refractive index n_r is greater or smaller than unity [25,37]. In our case, the dark hollow region can be generated in the focal plane of the lens by an RSCV beam with a given topological charge m. Controlling the intensity distribution of coherent and partially coherent vortex beams was proposed as a means to trap small nanoparticles with the refractive index smaller than the one of the surrounding medium [37]. We now adopt the following parameter values: $\lambda = 632.8$nm, which is the carrier wavelength of an RSCV beam, $m = 1$, $I_0 = 1W/\text{mm}^2$, $\sigma_I = 8$mm, $a = 30$nm, $n_1 = 1$ (air bubble) and $n_2 = 1.33$ (water). Further, to attain sufficiently high RSCV beam intensities, the other parameters are taken as $l = 2.5$m and $f = 5$mm.

The RSCV beam intensity profiles have a circular symmetry in any transverse plane, resulting in the circularly symmetric radiation forces acting on a trapped nanoparticle. In Fig. 3, we display the density plots of the x-component of the gradient force $F_x(x, y = 0, z) = \mathbf{e}_x \cdot \mathbf{F}_{grad}(x, y = 0, z)$ and the magnitude of the scattering force $F_{scat}(x, y = 0, z)$ in the vicinity of the focal plane of the focusing lens. Further, we display in Fig. 4 the cross lines of $F_x(x, y = 0, z = f)$ and $F_{scat}(x, y = 0, z = f)$ of the RSCV beam in the focal plane. We consider three cases here: highly coherent RSCV source ($\sigma_c = 20$mm), moderately coherent RSCV source ($\sigma_c = 8$mm), and nearly incoherent RSCV source ($\sigma_c = 2$mm). As the gradient force is nearly three orders of magnitude greater than the scattering force, the latter is virtually negligible in practice. With the coherence level of the beam decreasing from very high to very low, the gradient force changes rather insignificantly. Note that the positive value of F_x corresponds to the x-component of the gradient force in the positive x direction. It can be inferred from Fig. 4 that there exists only one stable equilibrium position, labelled by a solid black dot in Fig. 4, for any trapped particle in a transverse plane of any RSCV beam in the neighborhood of the focal plane. The said equilibrium positions are also denoted by dashed white lines in Fig. 3.

Optics EXPRESS

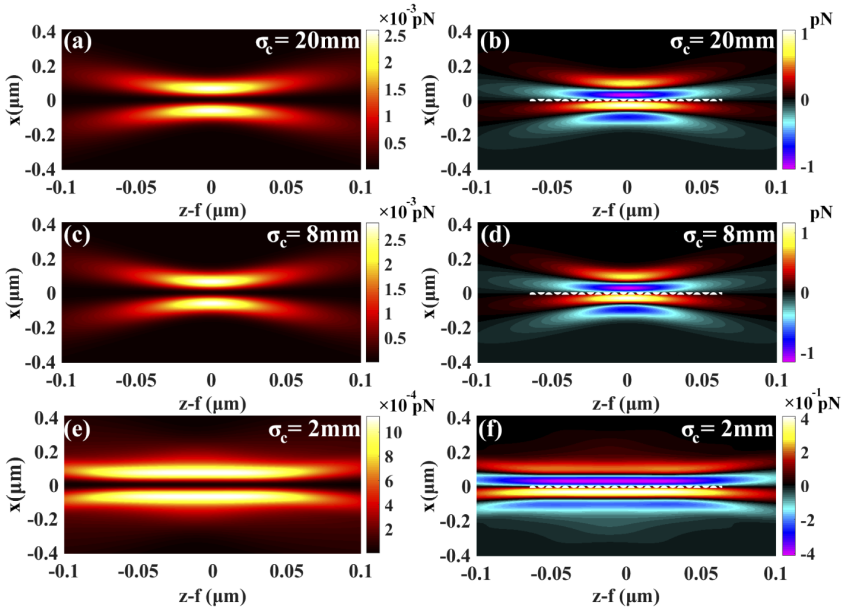

Fig. 3. Density plots of the magnitude of the scattering force $F_{scat}(x, y = 0, z)$ (left column) and the x-component of the gradient force $F_x(x, y = 0, z)$ (right column) exerted by a RSCV beam onto a small Rayleigh nanoparticle with the relative refractive index $n_r = 1/1.33$ in the vicinity of the focal plane for a variable source coherence width σ_c.

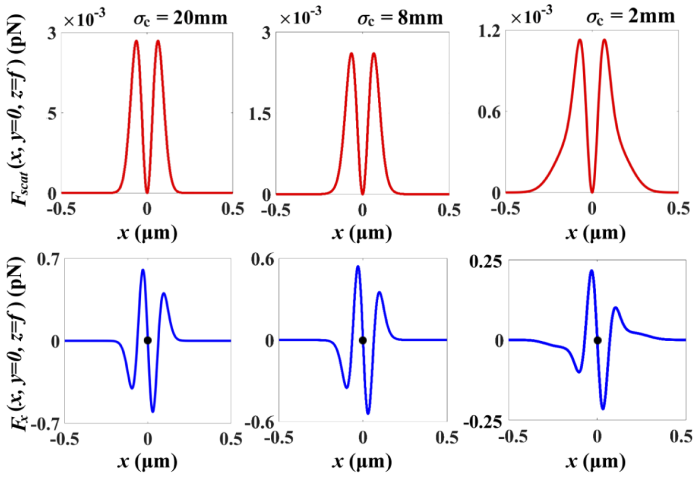

Fig. 4. Cross lines of the magnitude of the scattering force $F_{scat}(x, y = 0, z = f)$ (red curves) and x-component of the gradient force $F_x(x, y = 0, z = f)$ (blue curves) exerted by a RSCV beam onto a small Rayleigh nanoparticle with the relative refractive index $n_r = 1/1.33$ in the focal plane for a variable source coherence width σ_c.

Optics EXPRESS

Our theoretical and numerical results imply that we can indeed combine the advantages of low spatial coherence of the source and a stable vortex structure of the generated beam to ensnare a small particle by an RSCV beam that will be relatively stable to inevitable fluctuations in a surrounding medium. Thus, RSCV beams of **any spatial coherence level** can trap nanoparticles, made of a material with the refractive index smaller than the one of the surrounding medium, in any transverse plane in the vicinity of the focal plane. Finally, we note that the magnitudes of the gradient and scattering forces drastically decrease for the vortex beams with topological charges $m>1$ in agreement with previously published results [37].

5. Summary

In this work, we have established, for the first time to our knowledge, a general form of the cross-spectral density function of partially coherent sources generating vortex beams that maintain their vortices on propagation through any linear ABCD optical system, including free space and a thin optical lens. To illustrate our general results, we introduced a new class of partially coherent vortex beams with a closed form cross-spectral density function at the source. We demonstrated through numerical simulations that each member of the new class of vortex endowed beams maintains its vortex structure on propagation through an ABCD system regardless of the source state of spatial coherence. As well we showed that the vortex preserving partially coherent beams can be used in particle trapping applications by determining the radiation and scattering forces exerted by any such beam onto a small Rayleigh particle. Instructively, the vortex structure preservation of the new beams implies that novel beams of a very low state of coherence, which are highly stable to intrinsic environment fluctuations, can be employed to trap Rayleigh nanoparticles with the refractive index smaller than that of a surrounding medium.

Funding

National Key Research and Development Program of China (2019YFA0705000); National Natural Science Foundation of China (11525418, 11874046, 11904247, 11947239, 11974218, 91750201); Natural Sciences and Engineering Research Council of Canada (RGPIN-2018-05497); Innovation group of Jinan (2018GXRC010); China Postdoctoral Science Foundation (2019M662424).

Disclosures

The authors declare no conflicts of interest.

References

1. P. Coullet, L. Gil, and F. Rocca, "Optical vortices," Opt. Commun. **73**(5), 403–408 (1989).
2. L. Allen, M. W. Beijersbergen, R. J. C. Spreeuw, and J. P. Woerdman, "Orbital angular momentum of light and the transformation of Laguerre-Gaussian laser modes," Phys. Rev. A **45**(11), 8185–8189 (1992).
3. Y. Shen, X. Wang, Z. Xie, C. Min, X. Fu, Q. Liu, M. Gong, and X. Yuan, "Optical vortices 30 years on: OAM manipulation from topological charge to multiple singularities," Light: Sci. Appl. **8**(1), 90 (2019).
4. C. Qiu and Y. Yang, "Vortex generation reaches a new plateau," Science **357**(6352), 645 (2017).
5. H. He, M. E. J. Friese, N. R. Heckenberg, and H. Rubinsztein-Dunlop, "Direct observation of transfer of angular momentum to absorptive particles from a laser beam with a phase singularity," Phys. Rev. Lett. **75**(5), 826–829 (1995).
6. D. G. Grier, "A revolution in optical manipulation," Nature **424**(6950), 810–816 (2003).
7. N. Bozinovic, Y. Yue, Y. Ren, M. Tur, P. Kristensen, H. Huang, A. E. willner, and S. Ramachandran, "Terabit-scale orbital angular momentum mode division multiplexing in fibers," Science **340**(6140), 1545–1548 (2013).
8. D. Ding, W. Zhang, Z. Zhou, S. Shi, G. Xiang, X. Wang, Y. Jiang, B. Shi, and G. Cuo, "Quantum storage of orbital angular momentum entanglement in an atomic ensemble," Phys. Rev. Lett. **114**(5), 050502 (2015).
9. F. Tamburini, G. Anzolin, G. Umbriaco, A. BianChini, and C. Barbieri, "Overcoming the Rayleigh criterion limit with optical vortices," Phys. Rev. Lett. **97**(16), 163903 (2006).
10. J. Zeng, R. Lin, X. Liu, C. Zhao, and Y. Cai, "Review on partially coherent vortex Beams," Front. Optoelectron. **12**(3), 229–248 (2019).

Optics EXPRESS

11. X. Liu, L. Liu, Y. Chen, and Y. Cai, "Partially coherent vortex beam: from theory to experiment," *Vortex Dynamics and Optical Vortices*, H. Pérez-de-Tejada, ed. (InTech-open science, 2017), Chap.11, pp. 275–296.
12. G. Gbur, "Partially coherent beam propagation in atmospheric turbulence (invited)," J. Opt. Soc. Am. A **31**(9), 2038–2045 (2014).
13. X. Lu, Y. Shao, C. Zhao, S. Konijnenberg, X. Zhu, Y. Tang, Y. Cai, and H. P. Urbach, "Noniterative spatially partially coherent diffractive imaging using pinhole array mask," Adv. Photonics **1**(01), 1 (2019).
14. D. M. Palacios, I. D. Maleev, A. S. Marathay, and G. A. Swartzlander Jr., "Spatial correlation singularity of a vortex field," Phys. Rev. Lett. **92**(14), 143905 (2004).
15. Y. Yang, M. Mazilu, and K. Dholakia, "Measuring the orbital angular momentum of partially coherent optical vortices through singularities in their cross-spectral density functions," Opt. Lett. **37**(23), 4949–4951 (2012).
16. Y. Yang and Y. Liu, "Measuring azimuthal and radial mode indices of a partially coherent vortex field," J. Opt. **18**(1), 015604 (2016).
17. S. A. Ponomarenko, "A class of partially coherent beams carrying optical vortices," J. Opt. Soc. Am. A **18**(1), 150–156 (2001).
18. G. V. Bogatyryova, C. V. Felde, P. V. Polyanskii, S. A. Ponomarenko, M. S. Soskin, M. S. Soskin, and E. Wolf, "Partially coherent vortex beams with a separable phase," Opt. Lett. **28**(11), 878–880 (2003).
19. A. S. Ostrovsky, J. Garcia-Garcia, C. Rickenstorff-Parrao, and M. A. Olvera-Santamaria, "Partially coherent diffraction-free vortex beams with a Bessel-mode structure," Opt. Lett. **42**(24), 5182–5185 (2017).
20. S. A. Ponomarenko, "Complex Gaussian representation of statistical pulses," Opt. Express **19**(18), 17086–17091 (2011).
21. L. Ma and S. A. Ponomarenko, "Optical coherence gratings and lattices," Opt. Lett. **39**(23), 6656–6659 (2014).
22. L. Ma and S. A. Ponomarenko, "Free-space propagation of optical coherence lattices and periodicity reciprocity," Opt. Express **23**(2), 1848–1856 (2015).
23. Y. Chen, S. A. Ponomarenko, and Y. Cai, "Experimental generation of optical coherence lattices," Appl. Phys. Lett. **109**(6), 061107 (2016).
24. S. Yang, S. A. Ponomarenko, and Z. Chen, "Coherent pseudo-mode decomposition of a new partially coherent source class," Opt. Lett. **40**(13), 3081–3084 (2015).
25. R. Martínez-Herrero, G. Piquero, J. C. González de Sande, M. Santarsiero, and F. Gori, "Besinc pseudo-Schell model sources with circular coherence," Appl. Sci. **9**(13), 2716 (2019).
26. Y. Chen, S. A. Ponomarenko, and Y. Cai, "Self-steering partially coherent beams," Sci. Rep. **7**(1), 39957 (2017).
27. H. Mao, Y. Chen, C. Liang, L. Chen, Y. Cai, and S. A. Ponomarenko, "Self-steering partially coherent vector beams," Opt. Express **27**(10), 14353–14368 (2019).
28. S. A. Ponomarenko, W. Huang, and M. Cada, "Dark and antidark diffraction-free beams," Opt. Lett. **32**(17), 2508–2510 (2007).
29. X. Zhu, F. Wang, C. Zhao, Y. Cai, and S. A. Ponomarenko, "Experimental realization of dark and antidark diffraction-free beams," Opt. Lett. **44**(9), 2260–2263 (2019).
30. Y. Chen, A. Norrman, S. A. Ponomarenko, and A. T. Friberg, "Coherence lattices in surface plasmon polariton fields," Opt. Lett. **43**(14), 3429–3432 (2018).
31. H. Mao, Y. Chen, S. A. Ponomarenko, and A. T. Friberg, "Coherent pseudo-mode representation of partially coherent surface plasmon polaritons," Opt. Lett. **43**(6), 1395–1398 (2018).
32. S. A. Ponomarenko, "Self-imaging of partially coherent light in graded-index media," Opt. Lett. **40**(4), 566–568 (2015).
33. X. Liu, J. Yu, Y. Cai, and S. A. Ponomarenko, "Propagation of optical coherence lattices in the turbulent atmosphere," Opt. Lett. **41**(18), 4182–4185 (2016).
34. F. Wang, Y. Chen, L. Guo, L. Liu, and Y. Cai, "Complex Gaussian representations of partially coherent beams with nonconventional degrees of coherence," J. Opt. Soc. Am. A **34**(10), 1824–1829 (2017).
35. A. P. Prudnikov, Yu. A. Brychkov, and O. I. Marichev, *Integrals and Series* (Gordon and Breach, New York, 1992).
36. Y. Harada and T. Asakura, "Radiation forces on a dielectric sphere in the Rayleigh scattering regime," Opt. Commun. **124**(5-6), 529–541 (1996).
37. C. Zhao and Y. Cai, "Trapping two types of particles using a focused partially coherent elegant Laguerre-Gaussian beam," Opt. Lett. **36**(12), 2251–2253 (2011).